Cone algorithm jets in e^+e^- collisions

Junegone Chay*
Department of Physics, Korea University, Seoul 136-701, Korea

Stephen D. Ellis†
Department of Physics, FM-15, University of Washington, Seattle, Washington 98195
(Received 30 July 1996)

The structure of hadronic jets depends not only on the dynamics of QCD but also on the details of the jet finding algorithm and the physical process in which the jet is produced. To study these effects in more detail we calculate the jet cross section and the internal jet structure in e^+e^- annihilations and compare them to the results found in hadronic collisions using the *same* jet definition, the cone algorithm. The different structures of the overall events in the two cases are evident in the comparison. For a given cone size and jet energy, the distribution of energy inside the cone is more concentrated near the center for jets from e^+e^- collisions than for jets from hadronic collisions. [S0556-2821(97)02405-3]

PACS number(s): 13.87.−a, 12.38.Bx, 12.38.Qk

I. INTRODUCTION

Jets of narrowly collimated energetic hadrons are clearly seen in high energy collisions. They are observed in $p\bar{p}$ collisions [1] (CERN, Fermilab), in deep inelastic ep scattering [2] [DESY ep collider (HERA)], and in e^+e^- annihilations [3] (SLAC, CERN e^+e^- collider LEP, DESY, KEK). It is important to know how to analyze these jets quantitatively since they are essential not only for understanding and testing the underlying strong interaction theory but also in looking for new physics beyond the standard model such as the Higgs boson. The goal is to be able to employ the jets as surrogates for the underlying quarks and gluons to quantitatively characterize event structures in much the same way that leptons are used. Thus the main issue in studying jets is to reduce the various uncertainties, both theoretical and experimental.

The theoretical uncertainties in studying jets come from various sources. In the $p\bar{p}$ case the largest uncertainty comes from incomplete knowledge of the parton distribution functions, especially the gluon distribution function at small x. The jet cross section can vary by at least 10% when different sets of distribution functions are employed, although this situation is improving with time. Clearly, this uncertainty is absent in e^+e^- collisions. Second, there is uncertainty associated with the uncalculated higher-order corrections. This is illustrated by the fact that the theoretical cross section exhibits a dependence on the unphysical and arbitrary renormalization (factorization) scale μ. While the experimental jet cross section is, of course, independent of this scale, the residual dependence in the fixed-order perturbative result is a remnant of the truncation of the perturbative expansion.

Calculations [4,5] have been performed using the matrix elements at next-to-leading order [6] in $p\bar{p}$ collisions. When the next-to-leading order terms are included, the dependence of the cross section on the renormalization scale is markedly reduced, suggesting an uncertainty of order 10% due to the uncalculated higher-order corrections. For e^+e^- collisions the situtation is somewhat different. At lowest order (α_s^0) there is no μ dependence. Only at order α_s^1, as addressed here, does μ dependence appear. At this order there can be no cancellation of the μ dependence with higher orders. However, for the issue of the internal structure of jets, the real focus of this study, the dependence on μ should be comparable in the two cases, $p\bar{p}$ at order α_s^3 and e^+e^- at order α_s^1. In both cases the structure is evaluated at lowest nontrivial order.

Another important source of uncertainty arises from the use of different theoretical and experimental jet definitions. We can obtain an appreciation of this issue by considering the following qualitative pictures for jet production. In $p\bar{p}$ collisions, two of the partons in the incoming hadrons undergo a hard scattering producing final-state partons with large momenta transverse to the beam direction. The scattered partons can radiate further partons both after the hard scattering, final-state radiation, and before the scattering, initial-state radiation. The hard scattering process is also immersed in the background that arises from the interactions of the spectator partons. This underlying event is not part of the hard scattering but does contribute to the overall event. The partons from all of these sources then participate in the less-well-understood process of fragmentation into hadrons and can participate in the formation of a jet.

In e^+e^- collisions, electrons and positrons annihilate to produce initially a small number of energetic partons. These partons then radiate more partons that all fragment into hadrons that can be associated with jets. Since there are no incoming partons, the initial-state radiation and the background due to the spectator partons are absent. In both kinds of collisions the issues of color and energy-momentum conservation ensure that the fragmentation process into hadrons is a collective one with large numbers of partons acting coherently. Thus there can be no unique identification of a set of hadrons or a jet with a single scattered parton. Since there is no unique *a priori* jet definition for combining the final

*Electronic address: chay@kupt.korea.ac.kr
†Electronic address: ellis@phys.washington.edu

particles to form a jet, there is an arbitrariness in the choice of jet algorithm and different choices produce different results for the same process.

The dependence of jet cross sections on the jet definition is an issue both for comparing different experiments and for comparing experiment to theory. Precise comparisons are possible only if the detailed dependence on the jet definition exhibited in the data is reproduced by the theory. This is a limitation of the Born level calculation, which has only one parton per jet, thus exhibiting no structure to the jet at all. In Monte Carlo simulations the finite size of a jet arises from the subsequent showering of this parton and the nonperturbative fragmentation into hadrons. Both of these features contribute to the theoretical uncertainty. The inclusion of higher-order corrections reduces this uncertainty in the jet definition dependence because we can see nontrivial jet structure in the perturbative calculation. However, there remain many questions about the contribution of the rest of the event to the jet and to the uncertainty in the cross section. The interplay of the jet definition with the initial-state radiation and the underlying event can be studied by comparing two jet samples, one from $p\bar{p}$ collisions and the other from e^+e^- annihilations, where these two contributions are different. The goal is to generate experimental jet samples from e^+e^- events that can be directly compared with those from hadronic collisions. In this paper we compare the theoretical results for jets in e^+e^- and $p\bar{p}$ collisions using the same jet definition in each case.

In Sec. II, we discuss kinematic differences in e^+e^- collisions and $p\bar{p}$ collisions. In Sec. III, we define a jet in e^+e^- and hadronic collisions. In Sec. IV, the characteristics of the jet cross section in e^+e^- collisions are discussed. We compare the transverse energy distribution of the jets in e^+e^- and hadronic collisions in Sec. V. In the final section, we summarize the features of jets in both cases.

II. KINEMATIC DIFFERENCES

Let us first consider the kinematic differences in e^+e^- collisions and $p\bar{p}$ collisions. In the e^+e^- case, the center-of-mass energy of the partons participating in the hard scattering $\sqrt{\hat{s}}$ is fixed and equal to the total energy, $\sqrt{\hat{s}}=\sqrt{s}=Q$. Also, since the electrons and positrons have equal and essentially opposite momentum, the laboratory frame and the center-of-mass frame coincide. As a result the event structure is essentially spherical with respect to the interaction point and the detector geometry tends to exhibit the same symmetry. Generally, very simple jet definitions have been employed in e^+e^- experiments. For two-jet events, a jet is simply a hemisphere. For multijet events with a small number of jets simple invariant mass cuts have been used to define jets.

The $p\bar{p}$ case is more complex. The center-of-mass energy of the hard parton scattering is given by $\hat{s}=x_1x_2s$ where $\sqrt{s}$ is the center-of-mass energy of the beam particles and x_1 and x_2 are the fractions of the longitudinal momenta of the incoming hadrons carried by the scattering partons. Although the incoming hadrons have equal and opposite momenta, the scattered partons, in general, do not and the center-of-mass frame of the parton scattering is boosted along the beam direction with respect to the laboratory frame. Thus the relevant phase space is effectively cylindrical in the laboratory and the detectors for hadronic collider experiments are designed to match this symmetry. Likewise, the natural variable is the transverse energy E_T which is the component of the energy perpendicular to the beam axis and which is invariant under boosts along the beam direction. Since this characteristic is intrinsic to $p\bar{p}$ collisions, we have chosen to employ the jet definition of $p\bar{p}$ collisions both in e^+e^- and $p\bar{p}$ collisions to compare the jet samples in both cases.

An important kinematic difference between the e^+e^- and the $p\bar{p}$ cases arises from the fact, noted above, that in the e^+e^- case one performs experiments at fixed energy for the hard scattering, $\sqrt{s}=\sqrt{\hat{s}}$. Thus fixing the energy of a jet imposes a strong constraint on the rest of the hard scattering event and thus on the full final state. For example, if we fix the energy of the jet, we know how much energy associated with the hard scattering is outside the jet. However, this is not the case for hadronic collisions. Although we fix the energy of the jet, we do not know precisely how much energy associated with the hard scattering is outside the jet. The energy of the hard scattering process is $\sqrt{\hat{s}}=\sqrt{x_1x_2s}$ and depends on the specific x_i values and thus on the parton structure functions. In general, however, the distribution functions are rapidly falling functions of the x_i and $\sqrt{\hat{s}}$ will be only slightly larger, on average, than that necessary to generate the chosen jet. Another point is that, since we have chosen to impose the variable E_T on the e^+e^- case, we will have to integrate over the polar angle θ, or in the hadronic language the pseudorapidity $\eta=\ln\cot\theta/2$, in order to make E_T a free variable at lowest order. These differences in the kinematics will be important for understanding some of the ''trivial'' differences between the jets observed in the two types of experiments.

III. JET DEFINITION

Since jet cross sections critically depend on the jet definitions used, we can compare jet cross sections from different experiments only if we use the same jet definition for both of the jet samples. Thus we want to establish a standard jet definition. The point is not to select an optimal jet definition, since that will depend on specific applications, but to formulate a jet definition that satisfies reasonable criteria and can be used by both experimentalists and theorists to generate a sample of jets or jet cross sections for a wide range of processes that can be meaningfully compared between different groups. The relevant criteria are that the jet definition be easy to implement in all experiments and theoretical calculations, and yield reliable, finite results at any order in perturbation theory [7].

As discussed briefly above, the jet definition employed in practice in hadron collisions is characterized in terms of the transverse energy, $E_T=E\sin\theta$, measured inside a cone in η-ϕ space, where $\eta=\ln\cot\theta/2$ is the pseudorapidity and ϕ is the azimuthal angle around the beam direction. In terms of calorimeter cells i inside a cone defined by

$$\Delta R_i\equiv\sqrt{(\eta_i-\eta_J)^2+(\phi_i-\phi_J)^2}\leq R, \tag{1}$$

we define the transverse energy of the jet, E_T, as

$$E_T = \sum_{i \in \text{cone}} E_{T,i}. \tag{2}$$

The energy weighted direction of the jet is given by

$$\eta_J = \frac{1}{E_T} \sum_{i \in \text{cone}} E_{T,i}\eta_i \tag{3}$$

and

$$\phi_J = \frac{1}{E_T} \sum_{i \in \text{cone}} E_{T,i}\phi_i. \tag{4}$$

This procedure implies some number of iterations of the jet defining process in Eq. (1) until the quantities defined in Eqs. (2)–(4) are stable with the jet cone remaining fixed. We can also apply this jet definition at the parton level to form a jet. A single isolated parton with (E_T, η_J, ϕ_J) can be reconstructed as a jet. Or, two partons with $(E_{T,1}, \eta_1, \phi_1)$ and $(E_{T,2}, \eta_2, \phi_2)$ may be combined into a single jet. In that case the jet transverse energy is $E_T = E_{T,1} + E_{T,2}$, and $\eta_J = (E_{T,1}\eta_1 + E_{T,2}\eta_2)/E_T$, $\phi_J = (E_{T,1}\phi_1 + E_{T,2}\phi_2)/E_T$. To determine if the two partons are to be combined into a jet, we see if the two partons are in a cone of radius R about the jet axis. The condition that parton 1 fits into the cone is $(\eta_1 - \eta_J)^2 + (\phi_1 - \phi_J)^2 < R^2$, or

$$\frac{E_{T,2}}{E_{T,1} + E_{T,2}} |\mathbf{\Omega}_1 - \mathbf{\Omega}_2| < R, \tag{5}$$

where we denote a two-dimensional vector $\mathbf{\Omega} = (\eta, \phi)$. Similarly, the condition that parton 2 fits in the cone is

$$\frac{E_{T,1}}{E_{T,1} + E_{T,2}} |\mathbf{\Omega}_1 - \mathbf{\Omega}_2| < R. \tag{6}$$

Thus the combined condition is

$$|\mathbf{\Omega}_1 - \mathbf{\Omega}_2| < \frac{E_{T,1} + E_{T,2}}{\max(E_{T,1}, E_{T,2})} R. \tag{7}$$

If the two partons satisfy this condition, then we count one combined jet as specified above, but not the two one-parton jets. We can clearly generalize this definition to include more partons at higher orders.

This is the jet definition used for $p\bar{p}$ collisions in Ref. [4]. For the analysis described here, where we do not attempt to describe the experimental data, we neglect the subtleties of the jet merging problem and the parameter R_{sep} discussed in the last paper in Ref. [4]. A detailed comparison to data will be presented separately [8]. The precise definitions [9] used in the actual experiments are similar to the definition used here. Here, we apply this definition to calculating jet cross sections in e^+e^- events in order to compare to the $p\bar{p}$ case. As argued earlier, it is necessary to use the same definition of jets in comparing jets from different sources. We also define the kinematic variables $E_T = E\sin\theta$, the transverse energy perpendicular to the electron beam direction, η, the pseudorapidity, and ϕ, the azimuthal angle around the electron beam direction, in direct analogy to the $p\bar{p}$ case (even though it is less natural in the e^+e^- case).

IV. JET CROSS SECTION

We first consider the single inclusive jet cross section $d\sigma/dE_T$. Due to the kinematic constraints characteristic of e^+e^- collisions, this cross section exhibits a remarkable level of structure. As discussed above, we choose E_T as a variable instead of θ, the angle from the beam direction. The differential Born cross section $(d\sigma/dE_T)_B$ (normalized to two jets per event) is given by

$$\left(\frac{d\sigma}{dE_T}\right)_B = 48\pi\alpha^2 \sum_q e_q^2 \frac{E_T(1 - 2E_T^2/\hat{s})}{\hat{s}^2\sqrt{1 - 4E_T^2/\hat{s}}}, \tag{8}$$

where e_q is the quark charge, while the differential Born cross section $(d\sigma/d\Omega)_B$ for $e^+e^- \to q\bar{q}$ is well known as

$$\left(\frac{d\sigma}{d\Omega}\right)_B = \frac{3\alpha^2}{4\hat{s}} \sum_q e_q^2 (1 + \cos^2\theta). \tag{9}$$

At order α_s in e^+e^- collisions, nontrivial jet structure appears. We now include real gluon emission from a quark or an antiquark and virtual gluon corrections to quark-antiquark pair production. Final-state partons are combined to form a jet with a finite size according to the jet definition defined in the previous section. In the case of a three-parton final state the third parton can either be inside the detected jet or part of the system recoiling from the detected jet, which is constrained by energy-momentum conservation. To actually evaluate the cross section, we organize the calculation by adding and subtracting simplified matrix elements that have the correct divergences. The singular pieces are evaluated analytically and are explicitly canceled. The remaining finite integrals are evaluated numerically. At order α_s, the three partons are q, $\bar{q}$, and g and we label them as parton 1, 2, and 3, summing over all possible identifications with the three partons. We organize the calculation in such a way that parton 1 is opposite to the jet direction to balance momentum and conserve energy and parton 3 has the smallest transverse energy $(E_{T,1}, E_{T,2} > E_{T,3})$. There are three possibilities of forming a jet for the jet cone size $R < \pi/3$. Either parton 2 alone or parton 3 alone can form a jet, or partons 2 and 3 together form a jet. We choose the renormalization scale $\mu = E_T/2$ as suggested by the $p\bar{p}$ calculations [4].

Since we impose the jet algorithm, $d\sigma/dE_T$ depends on R as well as E_T. Let us first consider $d\sigma/dE_T$ versus E_T at fixed R. Figure 1 shows $d\sigma/dE_T$ at $R = 0.4$, 0.7, and 1.0, respectively, for $\sqrt{\hat{s}} = 50$ GeV along with the Born cross section $(d\sigma/dE_T)_B$. This choice of energy is essentially arbitrary except that it is large $(\sqrt{\hat{s}} \gg \Lambda_{\text{QCD}})$ and serves to remind us that we have included only photon exchange and not Z exchange. We expect that jet production from Z exchange is very similar to the case of photon exchange [10]. We also note that, except for the scale Λ_{QCD} in α_s, this theoretical cross section is scale-free. Results for other energies can be obtained (to a good approximation) by simply scaling the energy, keeping dimensionless ratios and angles fixed.

As is already evident in Eq. (8), the Born cross section diverges as $E_T \to \sqrt{\hat{s}}/2$ due to the Jacobian arising from the change of variables from $\cos\theta$ to E_T. As we increase the cone size, the cone tends to include more partons, thus more

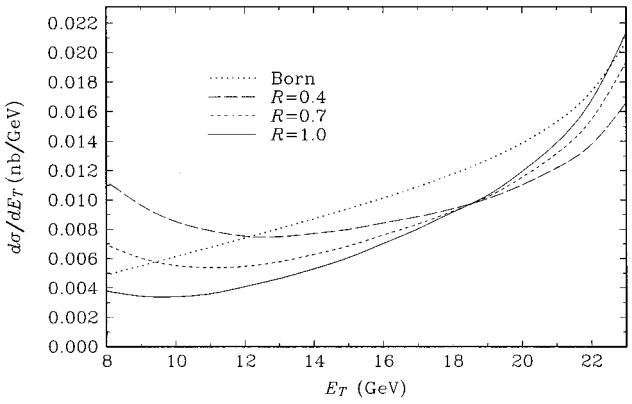

FIG. 1. $d\sigma/dE_T$ at order α_s with $\mu=E_T/2$ versus E_T at $\sqrt{\hat{s}}=50$ GeV in e^+e^- collisions for $R=$ 0.4, 0.7, and 1.0 and the Born cross section.

transverse energy inside the jet. Therefore the cross section increases for fixed E_T close to $\sqrt{\hat{s}}/2$ as we increase R, while it decreases for fixed E_T small compared to $\sqrt{\hat{s}}/2$ (i.e., it becomes more difficult to keep extra E_T out of the cone). As indicated in Fig. 1 the transition between the two types of behavior occurs for $E_T\simeq 19$ GeV or $x_T=2E_T/\sqrt{\hat{s}}\simeq 0.76$, where the cross section is essentially independent of R. This same feature is illustrated in Fig. 2 where the theoretical inclusive cross section for single jet production at order α_s is plotted as a function of the cone radius R for $E_T=10$, 19, and 23 GeV, respectively, with $\sqrt{\hat{s}}=50$ GeV. While the Born result is independent of R, the order-α_s cross section clearly depends on R, but with the form of the dependence varying with E_T. The slope with R is positive for large E_T, negative for small E_T, and approximately vanishes for $E_T\simeq 19$ GeV or $x_T\simeq 0.76$.

The general form of this dependence is approximately characterized by three parameters as

$$\frac{d\sigma}{dE_T}\approx a+b\ln R+cR^2. \tag{10}$$

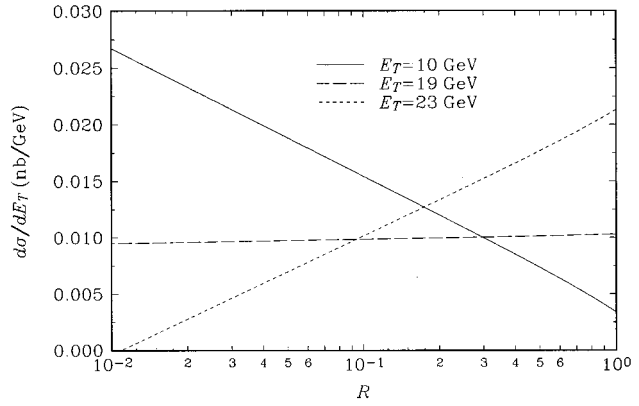

FIG. 2. $d\sigma/dE_T$ at order α_s with $\mu=E_T/2$ versus $\ln R$ at $\sqrt{\hat{s}}=50$ GeV, in e^+e^- collisions for $E_T=10$ GeV, 19 GeV, and 23 GeV.

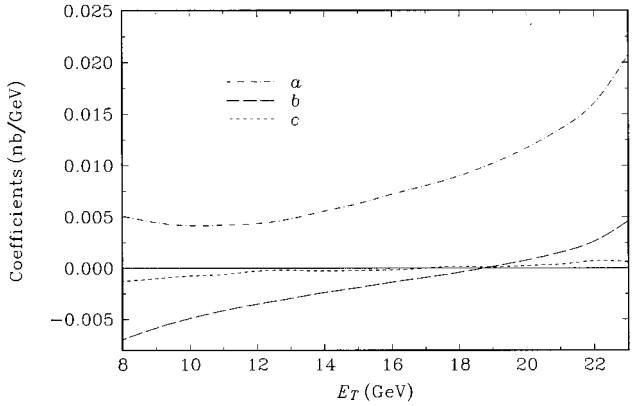

FIG. 3. Coefficients a, b, and c of Eq. (10) for e^+e^- collisions at $\sqrt{\hat{s}}=50$ GeV, as functions of E_T with $\mu=E_T/2$.

The numerical values and E_T dependence of the coefficients a, b, and c are indicated in Fig. 3 for $\sqrt{\hat{s}}=50$ GeV as in Figs. 1 and 2. We can think of the parameter a as describing the contribution of the two-parton final state, which is independent of R. Since this term is dominated by the Born cross section, its E_T dependence is easily understood by comparing with Fig. 1.

The form of the second term in Eq. (10) arises from the collinear divergence present in the perturbation theory at order α_s. The sign of b is negative for small E_T and it changes as we increase E_T. This behavior of b can be qualitatively understood using the results for the Sterman-Weinberg jet [11]. Sterman and Weinberg introduced a quantity $\sigma(\theta,\epsilon,\delta)$, which is the cross section for $e^+e^-\to qqg$ where a fraction $(1-\epsilon)$ of the total energy is emitted within two oppositely directed cones of half-angle δ, making an angle θ with the beam axis. Both ϵ and δ are very small. The result to order α_s is

$$\frac{d\sigma}{d\Omega}(\theta,\epsilon,\delta)=\left(\frac{d\sigma}{d\Omega}\right)_B\left[1-\frac{4\alpha_s}{3\pi}\left\{(3+4\ln 2\epsilon)\ln\delta+\frac{\pi^2}{3}-\frac{5}{2}\right\}+O(\epsilon,\delta)\right], \tag{11}$$

where $(d\sigma/d\Omega)_B$ is the Born differential cross section given in Eq. (9). We can transform Eq. (11) to $d\sigma/dE_T$ using the relation $E_T=E\sin\theta$. Note that the jet algorithm used by Sterman and Weinberg is different from the jet algorithm we use here. However, when δ and R are small, δ is proportional to R. Then, the coefficient of $\ln R$ is the same as the coefficient of $\ln\delta$.

For simplicity, let us consider the case in which θ approaches $\pi/2$ so that $E_T\to\sqrt{\hat{s}}/2$. Then, the relation between E_T and ϵ becomes $2E_T=(1-\epsilon)\sqrt{\hat{s}}\sin\theta\approx(1-\epsilon)\sqrt{\hat{s}}$. When we replace ϵ in Eq. (11) by $\epsilon\approx 1-2E_T/\sqrt{\hat{s}}$, we get

$$\frac{d\sigma}{dE_T}\approx\left(\frac{d\sigma}{dE_T}\right)_B\left[1-\frac{4\alpha_s}{3\pi}\left\{3+4\ln 2\left(1-\frac{2E_T}{\sqrt{\hat{s}}}\right)\right\}\ln R+\cdots\right], \tag{12}$$

where $(d\sigma/dE_T)_B$ is the Born cross section in Eq. (8) and the ellipsis represents the terms irrelevant to the coefficient of $\ln R$. Note that this only holds for small R and for $E_T \approx \sqrt{\hat{s}}/2$. However, as we can see in Fig. 2, the logarithmic dependence on R is sustained for large R. From Eq. (12), the point where the coefficient of $\ln R$ vanishes is given by $\ln(1-x_T) = -3/4 - \ln 2 = -1.44$ or $x_T \approx 0.76$, $E_T \approx 19$ GeV. Our numerical result shows that b vanishes for $E_T \approx 18.5$ GeV or $x_T \approx 0.74$, which is in (surprisingly) good agreement with this approximation. Said another way, we can understand the sign of b from the following considerations. The $\ln R$ term arises from the perturbative collinear singularity integrated over the angular phase space of the third parton. When this parton is inside the jet cone, R appears as the *upper* limit of the angular integral and the coefficient of $\ln R$ is positive. For the configuration with the third parton outside of the jet cone, R appears as the *lower* limit of the integral and $\ln R$ has a negative coefficient. For large E_T values the former situation dominates and $b > 0$, while for small E_T the latter configuration is more important and $b < 0$.

The coefficient c is, in some sense, a measure of the contribution from parts of the matrix element where the extra parton is essentially uncorrelated with the jet direction. This contribution should vary simply as the area of the cone, i.e., as R^2. We find that c in e^+e^- collisions is small in magnitude compared to that of a and also of b (and, in fact, is difficult to fit reliably with our numerical methods resulting in the small amplitude fluctuations in Fig. 3). The E_T variation of c is understood in essentially the same way as for b. Now the integral over the angular phase space for the third parton yields the two-dimensional area R^2 instead of $\ln R$. Thus, we expect the coefficients b and c to exhibit very similar behavior as functions of E_T. They are both negative at small E_T, positive at large E_T (i.e., $E_T \approx \sqrt{\hat{s}}/2$), and change sign at an intermediate E_T value. Our results suggest that they change sign at approximately the same x_T (E_T) value of about 0.75–0.8 ($E_T \approx 19$ GeV for $\sqrt{\hat{s}} = 50$ GeV). The vanishing of the R dependence at a specific E_T value was already apparent in Fig. 1. This structure appears to be characteristic of e^+e^-, at least in low order perturbation theory, and it will be interesting to check for it in the experimental data.

In hadronic collisions, the dependence on R can be approximated by the same form as in Eq. (10), but with different values of the coefficients. We expect the same form because the logarithmic term, which represents the collinear divergence at this order, appears regardless of what the beam particles are. This dependence is a general feature of the jet cross section in perturbation theory. However, the E_T behavior of the coefficients in $p\bar{p}$ collisions is expected to be quite different due to the kinematic differences between the e^+e^- and the $p\bar{p}$ cases that we discussed earlier. We expect that the coefficient b is always positive and does not vary much as we vary E_T in the $p\bar{p}$ case. This feature arises from the fact the partonic center-of-mass energy, $\sqrt{\hat{s}} (= \sqrt{x_1 x_2 s})$, is almost always just slightly larger than $2E_T$. This result is, in turn, ensured by the fact that the parton distribution functions are sharply peaked at small x. Therefore b is determined by the behavior of the cross section at $2E_T/\sqrt{\hat{s}} \approx 1$. It is obvious from the e^+e^- case that b should be positive in the $p\bar{p}$ case. The same argument also suggests that the coefficient c will be positive for all E_T in the $p\bar{p}$ case. Furthermore, the magnitude of c should be relatively larger in the $p\bar{p}$ case due to the contributions from the initial-state radiation that is present in this case. Since the initial-state radiation is correlated with the beam direction and not with the direction of the jet, the distribution of the partons from the initial-state radiation is rather isotropic with respect to the jet direction. Therefore the contribution of these partons to the cross section is proportional to the area of the jet cone R^2. In the experimental data from $p\bar{p}$ collisions one expects a further contribution to c from the essentially uncorrelated underlying event. It will be informative to characterize data from both e^+e^- and $p\bar{p}$ collisions in terms of the coefficients in Eq. (10).

TABLE I. Comparison of values for coefficients a, b, and c for both e^+e^- and $p\bar{p}$ collisions scaled by the relevant Born cross section. All calculations are for $\mu = E_T/2$ and $R_{\rm sep} = 2R$. The e^+e^- results are for $\sqrt{\hat{s}} = 50$ GeV while the $p\bar{p}$ numbers are for $\sqrt{\hat{s}} = 1800$ GeV.

Process	E_T(GeV)	$\frac{a}{(d\sigma/dE_T)_B}$	$\frac{b}{(d\sigma/dE_T)_B}$	$\frac{c}{(d\sigma/dE_T)_B}$
e^+e^-	10	0.68	−0.80	−0.12
e^+e^-	15	0.67	−0.20	−0.023
e^+e^-	18	0.77	−0.035	0.014
e^+e^-	20	0.86	0.056	0.017
e^+e^-	22	0.92	0.15	0.041
e^+e^-	23	1.01	0.22	0.030
$p\bar{p}$	100	0.74	0.18	0.27

The expectation that the $p\bar{p}$ jet cross section will increase rapidly with R is illustrated for one E_T value in Fig. 1 of the last paper in Ref. [4]. In the same paper an analysis in terms of Eq. (10) was carried out at $E_T = 100$ GeV (see Table I of that paper). To compare to the current study of theoretical cross sections, also with $\mu = E_T/2$ (and $R_{\rm sep} = 2R$), it is essential to scale out the overall differences between e^+e^- and $p\bar{p}$ by dividing out the Born cross section in each case. The resulting scaled coefficients for a sampling of E_T values are displayed in Table I. As expected, the $p\bar{p}$ coefficients are all positive, of order 1 and most closely resemble the e^+e^- numbers for large values of E_T. Note, in particular, the relatively good agreement of the a and b coefficients in the two processes for the largest e^+e^- E_T values. The relatively larger a coefficient in the e^+e^- case is suggestive of narrower (and thus relatively R-independent) jets in e^+e^- collisions as will be discussed below. Note also that the c coefficient is larger in the $p\bar{p}$ case by approximately an order of magnitude as expected due to the presence of uncorrelated initial-state radiation. Finally, recall from Ref. [4] that these theoretical results for $p\bar{p}$ are in approximate agreement with the experimental data. A more detailed theoretical comparison, including the effects of $R_{\rm sep}$ will be presented elsewhere [8]. Experimental studies over a broad E_T range would also be useful.

V. JET STRUCTURE

Now, let us turn to the interesting question of the internal structure of jets. In our idealized picture of the scattering

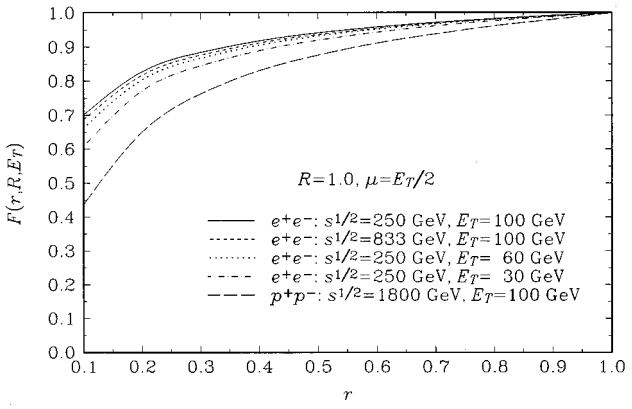

FIG. 4. $F(r,R,E_T)$, the fractional transverse energy distribution, for $r \leqslant 1.0$, $R=1.0$ for various processes and values of $\sqrt{\hat{s}}$ and E_T.

process, contributions to the energy in the jet cone arise from final-state radiation and, in the case of $p\bar{p}$ collisions, also from initial-state radiation and the underlying event. Since the latter two contributions are uncorrelated with the jet direction, we naively expect jets in $p\bar{p}$ collisions to exhibit a less correlated, broader internal energy distribution compared to that of e^+e^- jets. At the same time, in both hadronic and e^+e^- collisions, there is some energy that falls outside the cone that is correlated to the hard scattering. The higher-order calculation to first nontrivial order in α_s correctly includes the effect of the correlated energy that falls outside the cone. In the hadronic case, it also accounts for the fact that a large fraction of the energy far away from the jet is, in fact, correlated, corresponding to soft but correlated perturbative bremsstrahlung in the hard event [12].

It should be possible to confirm the validity of these ideas by studying in detail the structure within jets in both the theoretical results and in the experimental data. An example quantity is the transverse energy distribution within a jet. Defining a jet sample by a cone radius R and a total jet transverse energy E_T, we consider the fraction $F(r,R,E_T)$ of E_T that falls inside an inner cone defined by the radius r. This quantity is constrained at the boundaries to be $F(0,R,E_T)=0$ and $F(R,R,E_T)=1$. The theoretical results of the fraction $F(r,R,E_T)$ are illustrated in Fig. 4 corresponding to e^+e^- jet samples with a few different values of $\sqrt{\hat{s}}$ and E_T, and a hadronic jet sample with $\sqrt{s}=$ 1800 GeV, $E_T=$ 100 GeV. (The last values are intended to be physically relevant to Fermilab Tevatron data while the e^+e^- values are chosen for easy comparison to the hadronic results.) In both jet samples, the jet cone is fixed at $R=1.0$. Most of the energy falls in the small inner cone due to the collinear logarithmic contribution. If we use the Born terms alone, all the energy will be at $r=0$ and $F(r>0,R,E_T)=1$ everywhere else inside the jet cone. In contrast, the calculation at order α_s exhibits a nontrivial distribution, though there is still a (double) logarithmic singularity for $r \to 0$. By comparing these two samples of jets calculated from the theory, we can conclude that jets in e^+e^- collisions are narrower than jets in hadronic collisions. That is, the fact that $F_{e^+e^-} > F_{p\bar{p}}$ at all r (for $0<r<R$) means that the energy distribution inside of the jets in e^+e^- collisions is more concentrated near the center. Note that this theoretical analysis does not include the further broadening that is expected to arise from the underlying event contribution.

Figure 4 also illustrates that the jet shape in the e^+e^- jet sample varies systematically with E_T and $\sqrt{\hat{s}}$, becoming narrower with increasing E_T at fixed $\sqrt{\hat{s}}$ (compare $E_T=$ 30, 60, and 100 GeV at $\sqrt{\hat{s}}=$ 250 GeV), and broader with increasing $\sqrt{\hat{s}}$ at fixed E_T (compare $\sqrt{\hat{s}}=$ 250 and 833 GeV at $E_T=$ 100 GeV). But in the entire kinematic range, the jet from the e^+e^- collision is consistently narrower than the hadronic jet.

To understand these results in more detail it is helpful to consider the quantity $1-F(r,R,E_T)$, the distance *down* from the upper axis, which is the fraction of the transverse energy outside the smaller cone of radius r and inside the jet size R. At the order we calculate the jet cross section this quantity is proportional to $\alpha_s(\mu)$ evaluated at $\mu=E_T/2$ and is thus a decreasing function of E_T. This is directly illustrated by comparing the e^+e^- jet sample with $\sqrt{\hat{s}}=$ 833 GeV and $E_T=100$ GeV to the sample with $\sqrt{\hat{s}}=$ 250 GeV and $E_T=$ 30 GeV. In each sample the ratio $E_T/\sqrt{\hat{s}}=0.12$ is the same and the only difference is the value of $\alpha_s(E_T/2)$. Since $1-F(r,R,E_T)$ is proportional to $\alpha_s(E_T/2)$, the 20% difference in magnitudes of this quantity for the two samples arises from the ratio of $\alpha_s(50\ \text{GeV})$ to $\alpha_s(15\ \text{GeV})$.

When we compare e^+e^- jets to $p\bar{p}$ jets in Fig. 4, we find that the quantity $1-F(0.5,1.0,100\ \text{GeV})$ is about two times smaller for the former type of collision. Again, this illustrates that the transverse energy is more concentrated near the center for a jet from an e^+e^- collision than that for a jet from a hadronic collision. In these theoretical calculations this feature arises from two primary differences in the two kinds of collisions. First, the initial-state radiation from the beam hadrons in the hadronic case is absent in the e^+e^- case. Though the partons produced in the initial-state radiation are uncorrelated with the direction of the final jets, they can come into the jet cone and contribute to a broad jet energy distribution. The second point that contributes to the narrower jets in the e^+e^- sample is that, at order α_s, the e^+e^- sample is dominated by naturally narrower ''quark jets,'' consisting of a quark plus a gluon. By comparison the hadronic sample also includes a large component of broader ''gluon jets,'' consisting of two gluons (or a quark-antiquark pair in the color octet state).

An interesting feature of the event structure correlated with jets shows up when we consider the region $r>R$ as illustrated in Fig. 5. In this region the quantity $F(r,R,E_T)-1$ measures how much correlated energy falls outside the jet. Recall that $F(r,R,E_T)$ is the E_T inside a cone of radius r normalized to the fixed jet E_T in the cone of radius R. Thus the fractional E_T *outside* of the jet is given by $F(r,R,E_T)-F(R,R,E_T)=F(r,R,E_T)-1$. The correlated energy outside the jet cone comes from the partons produced after the hard scattering for both the e^+e^- and the $p\bar{p}$ cases, and from those produced in the initial-state radiation before the hard scattering for the $p\bar{p}$ case. The jet algorithm does not distinguish where the partons come from. It simply tries to identify clusters of the partons that satisfy the criteria to form a jet. Based on the arguments used earlier, we might

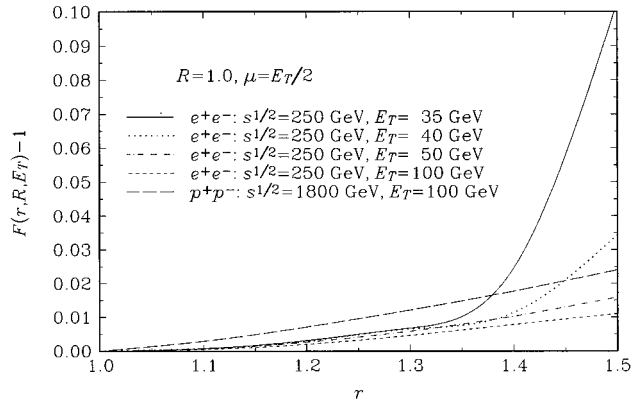

FIG. 5. $F(r,R,E_T)-1.0$, the fractional transverse energy distribution, for $r \geqslant 1.0$, $R=1.0$ for various processes and values of E_T.

naively expect that the energy outside of the cone in the hadronic case is larger than that in the e^+e^- case, since the hadronic collision contains also the essentially isotropic initial-state radiation contribution. However, due to the kinematic differences in the two situations, this simple expectation is not always realized. The behavior for the e^+e^- case depends strongly on the jet energy E_T. When E_T is small compared to the fixed value of $\sqrt{\hat{s}}$, $F(r,R,E_T)$ outside of the jet cone is necessarily large due to energy-momentum conservation.

As indicated in Fig. 5, $F(r,R,E_T)-1$ for the e^+e^- case for $r>R$ with $\sqrt{\hat{s}}=$ 250 GeV, remains small with small slope for $E_T \geqslant 50$ GeV but becomes a rapidly increasing function of r for $E_T<40$ GeV. The slope with r systematically increases with decreasing E_T. It turns out that the behavior outside the jet for the hadronic jet sample does not vary much as we vary E_T and the magnitude remains small (as indicated for the single E_T value shown). This relative independence of E_T arises from a feature already discussed. Since parton distribution functions are peaked at small values of x, $\sqrt{\hat{s}}$ is constrained to remain near its minimum value, $2E_T$, and the invariant mass squared of the final state resulting from the hard scattering stays small. If a parton outside the jet has appreciable energy, this would require a large invariant mass for the system composed of that parton and the partons inside the jet. Therefore, if there is a parton outside of the jet, the energy of that parton tends to be small to make the combined invariant mass small. As an example, the hadronic case with $\sqrt{s}=$ 1800 GeV, $E_T=$ 100 GeV is shown in Fig. 5.

Note that the transverse energy deposited just outside the jet cone is very small in all cases. This feature is due to the jet algorithm itself. The jet algorithm tries to include as many partons as possible as long as the criteria for jet formation, Eq. (7), are satisfied. During the jet finding process, the jet cone will tend to adjust its position in order to ''pull'' partons just outside of the cone into the cone. In this way the E_T inside the cone is increased. This effect will play no role only when the parton just outside the cone has vanishingly small E_T. Therefore the transverse energy just outside the jet cone is very small in all cases. Of course, this feature is likely to be reduced by the largely uncorrelated, uniformly distributed contributions of the underlying event in the $p\bar{p}$ case and parton fragmentation effects in both $p\bar{p}$ and e^+e^- collisions.

VI. CONCLUSION

The analysis of the inclusive jet cross section in e^+e^- collisions and in $p\bar{p}$ collisions, including the next-order contributions, has achieved a high level of sophistication. It is important that we further improve our understanding of physical processes involving jets so that we can use the jets as event tags to search for new physics. An essential issue is the systematic uncertainty that arises from the role played by the underlying event in processes involving hadrons in the initial state. To study this issue an important tool is the comparison of jets from different types of events where the underlying event is different. However, to study systematic effects of the jets in more detail, it is necessary to compare jet samples with the *same* jet definition from the full range of possible processes, $p\bar{p}$ collisions, e^+e^- annihilations, and ep scattering.

Here, we have theoretically evaluated the jet cross section in both e^+e^- and $p\bar{p}$ collisions employing the same cone style jet algorithm and have discussed the internal structure of the jets. By comparing theoretical jet cross sections from hadron collisions and e^+e^- annihilations, we note differences in the global dependence of the jet cross sections on the jet size R and in the distribution of the transverse energy inside the jets. In particular, the jet cross section is expected to be a monotonically increasing function of R for hadronic collisions while in e^+e^- collisions the cross section is expected to increase with R at large x_T and decrease with R at small x_T. However, in both cases we expect the R dependence to exhibit the simple structure shown in Eq. (10), only the specific values of the coefficients will differ. Perturbative QCD theory also predicts that the jets in e^+e^- collisions are narrower than those produced in hadronic collisions in the sense that the distribution of the transverse energy inside the jet is more concentrated near the center in e^+e^- collisions. This difference has already been observed in a careful comparison of e^+e^- and $p\bar{p}$ jet data performed by the OPAL Collaboration [13]. In the current theoretical analysis these differences in jet cross sections and jet structures arise from the different kinematics discussed in Sec. II, the presence of the initial-state radiation in $p\bar{p}$ collisions, and the different mix of jet-type (gluon versus quark) in the different processes. A more thorough comparison of theory with data will be presented elsewhere [8].

The calculation of the theoretical jet cross section for ep scattering is also in progress and it will be interesting to compare all the jet cross sections from all of the available sources of jets with the same jet definition. The case of ep scattering is expected to exhibit characteristics in between the e^+e^- and the $p\bar{p}$ cases since there is only a single hadron to serve as the source of the initial-state radiation and the underlying event. However, as with the e^+e^- case, we have to be careful about the kinematics. For example, we have to

identify the energetic outgoing electrons to ensure that only photons and neutral weak Z bosons are exchanged between the electron and the proton. We hope that the comparison among these different jet samples will deepen our understanding of the interplay of jet definitions with initial-state radiation and the underlying event as well as enhance our understanding of how different kinematic situations affect the jet cross sections.

ACKNOWLEDGMENTS

This work was supported by the U.S. Department of Energy under Grant No. DE-FG06-91ER40614. One of the authors (J.C.) was supported in part by KOSEF Grant No. 941-0200-02202, Ministry of Education BSRI 94-2408, and the Korea Science and Engineering Foundation through the SRC program of SNU-CTP. One of us (S.D.E.) thanks J. W. Gary for several helpful discussions.

[1] See, for example, CDF Collaboration, F. Abe *et al.*, Phys. Rev. Lett. **68**, 1109 (1992); **70**, 713 (1993); **70**, 1376 (1993).

[2] See, for example, ZEUS Collaboration, Phys. Lett. B **306**, 158 (1993); Z. Phys. C **59**, 231 (1993).

[3] See, for example, T. Hebbeker, in *Proceedings of the Joint International Lepton-Photon Symposium and Europhysics Conference on High Energy Physics*, Geneva, Switzerland, 1991, edited by S. Hegarty *et al.* (World Scientific, Singapore, 1992), Vol. 2, p. 73.

[4] S.D. Ellis, Z. Kunszt, and D.E. Soper, Phys. Rev. Lett. **62**, 726 (1989); Phys. Rev. D **40**, 2188 (1989); Phys. Rev. Lett. **64**, 2121 (1990); **69**, 3615 (1992).

[5] F. Aversa, P. Chiappetta, M. Greco, and J. Ph. Guillet, Phys. Lett. B **210**, 225 (1988); **211**, 465 (1988); Nucl. Phys. **B327**, 105 (1989); Z. Phys. C **46**, 235 (1990); **49**, 459 (1990); Phys. Rev. Lett. **65**, 401 (1990).

[6] R.K. Ellis and J.C. Sexton, Nucl. Phys. **B269**, 445 (1986).

[7] See, for example, J. E. Huth *et al.*, in *Research Directions for the Decade*, Proceedings of the Summer Study on High Energy Physics, Snowmass, Colorado, 1990, edited by E. L. Berger (World Scientific, Singapore, 1991).

[8] J. Chay, S.D. Ellis, and J. Park (in preparation).

[9] For a compilation of jet algorithms, see B. Flaugher and K. Meier, in *Research Directions for the Decade* [7].

[10] L.S. Brown and S. Li, Phys. Rev. D **26**, 570 (1982).

[11] G. Sterman and S. Weinberg, Phys. Rev. Lett. **39**, 1436 (1977).

[12] G. Marchesini and B.R. Webber, Phys. Rev. D **38**, 3419 (1988).

[13] OPAL Collaboration, R. Akers *et al.*, Z. Phys. C **63**, 197 (1994).